Available online at www.sciencedirect.com
ScienceDirect
Journal of Molecular Catalysis A: Chemical 272 (2007) 182–190
JOURNAL OF MOLECULAR CATALYSIS A: CHEMICAL
www.elsevier.com/locate/molcata

Effect of reaction conditions on the catalytic performance of Fe-Mn catalyst for Fischer-Tropsch synthesis

Ying Liu [a,b], Bo-Tao Teng [a,c], Xiao-Hui Guo [a,b], Ying Li [a], Jie Chang [a], Lei Tian [a,b], Xu Hao [a,b], Yu Wang [a,b], Hong-Wei Xiang [a], Yuan-Yuan Xu [a], Yong-Wang Li [a,*]

[a] *State Key Laboratory of Coal Conversion, Institute of Coal Chemistry, Chinese Academy of Sciences, Taiyuan 030001, PR China*
[b] *Graduate University of Chinese Academy of Sciences, Beijing 100039, PR China*
[c] *Zhejiang Key Laboratory for Reactive Chemistry on Solid Surfaces, Institute of Physical Chemistry, Zhejiang Normal University, Jinhua 321004, PR China*

Received 19 December 2006; received in revised form 16 March 2007; accepted 20 March 2007
Available online 24 March 2007

Abstract

The effects of reaction conditions on the performance of an Fe-Mn catalyst for Fischer-Tropsch synthesis (FTS) have been investigated in a continuous spinning basket reactor. Experiments were carried out under a wide range of industrially relevant reaction conditions including reaction temperature of 533–573 K, pressure of 0.93–2.96 MPa, inlet H_2/CO molar ratio of 0.80–2.50 and space velocity of $(0.46–1.85) \times 10^{-3}$ N m^3 kg$_{cat}^{-1}$ s^{-1}. The selectivities to low molecular weight hydrocarbons basically increased with the increase of reaction temperature, total pressure and inlet H_2/CO ratio, except for ethylene. The FTS reaction rate and the overall oxygenates formation rate increased with increasing reaction temperature, pressure, space velocity and H_2/CO ratio on the whole. It was found that the catalyst has relatively high activity and selectivity in producing light alkenes. It also exhibited excellent stability during the 700 h run at H_2/CO ratio of 1.00, which indicates that the catalyst has good longevity and is suitable for syngas derived from coal with low H_2/CO ratio to produce light olefins and high-quality liquid fuels. Meanwhile, it may have potential promising applications in advanced stirred tank slurry reactors. In addition, the detailed investigation of FTS reaction performance for the Fe-Mn catalyst can provide full and accurate basic information for industrial scale-up.

Keywords: Fischer-Tropsch synthesis; Fe-Mn catalyst; Hydrocarbon selectivity; Oxygenate

1. Introduction

The synthesis of liquid fuels from coal-derived syngas via Fischer-Tropsch synthesis (FTS) reaction is one of the most important processes to solve the shortage of transport fuels [1–3]. In the FTS process, the conversion of syngas over a catalyst is one of the most pivotal steps. Consequently, choosing a suitable catalyst is very important. Iron-based catalysts have been used as commercial catalysts for FTS to produce a wide range of paraffin and olefin products, ranging from methane to high molecular weight waxes [4,5]. The Fe-Mn catalyst, as one of the most important catalyst systems, has received extensive attention in recent years because of the higher olefin and middle distillation cut selectivities which allow their products to be used as a feedstock for the chemical industry [6–12]. Therefore, the Fe-Mn catalyst has a promising industrial application.

Investigative results in the literature show that syngas conversion on iron catalysts which are promoted with large amounts of oxides, yield unusually high selectivity to C_2–C_4 olefins and suppress methane formation [13–16]. Several researchers also studied various Fe-Mn matrix catalysts [6,7,15,17–21]. Maiti et al. [6,7] studied a series of Fe-Mn catalysts and found that the catalyst with low Mn content and a high degree of reduction has higher activity during the initial period of the run process, and the small amounts of Mn can enhance the formation of olefin products, while the catalyst with a higher content of Mn has relatively stable activity under high temperature reduction. Barrault et al. [15] found that there is considerable interaction between iron and manganese. Moreover, when there are small quantities of sulphate salt in iron or iron-manganese supported catalysts, electronic changes in metal atoms induced by surrounding man-

* Corresponding author. Tel.: +86 351 7560831; fax: +86 351 7560668.
E-mail addresses: yliu506@hotmail.com (Y. Liu), ywl@sxicc.ac.cn (Y.-W. Li).

1381-1169/$ – see front matter © 2007 Elsevier B.V. All rights reserved.
doi:10.1016/j.molcata.2007.03.046

ganese compounds and/or S atoms and the formation of surface sulphide also influence the activity and selectivity, especially the olefin formation. However, van Dijk et al. [22], in their studies of Fe-Mn catalysts with various manganese contents, showed that no relationship exists between the olefin selectivity and the amount of manganese added. Furthermore, the fully carburized Fe-Mn catalyst obeyed an ASF distribution, which was quite similar to that of a carburized iron catalyst without manganese oxide.

Zhong et al. [23] exploited a novel Fe-Mn catalyst, which had been prepared by a special degradation method. This catalyst shows good activity and stability in the fixed bed reactor and the slurry phase reactor [24,25]. It is well known that the higher FTS activity of the Fe-Mn catalyst in a fixed-bed reactor would result in much higher H_2/CO in the outlet than that in the inlet due to the integral effect, which might have distorted the significant kinetic information. Meanwhile, the mixture of products with different time accumulation in a slurry reactor also leads to difficulties for the understanding of reaction condition effects on FTS reaction performance. Therefore, the two kinds of reactors are not much suitable for the detailed investigation of FTS at various reaction conditions although they can provide beneficial information for the evaluation of different catalysts. Considering that the reaction environment is uniform and the products are easily collected and analyzed in a continuous spinning basket reactor, it can provide more favorable information for the understanding of FTS reaction performance with the variation of reaction conditions.

The main objective of this work is to systematically examine the catalytic performance of the Fe-Mn catalyst in a spinning basket reactor and compare it with that in a fixed bed reactor.

2. Experimental

2.1. Catalyst and reduction

The Fe-Mn catalyst used in this study was prepared by the Institute of Coal Chemistry (ICC), Chinese Academy of Sciences, and it had undergone pilot-scale tests in the fixed bed reactor in the industrial center of ICC. The preparation method has been patented [23]. The catalyst was prepared from Fe-Mn oxalate by a special controlled degradation method, and some open information can be found in the literature [23,26]. The catalyst is mainly composed of the active components of Fe and Mn (atomic ratio of Fe/Mn is 3), and 1 wt% of K_2O. The BET surface area of the fresh catalyst was 117.8 m^2/g. The average particle size of the catalyst that was evidenced by TEM and small angle X-ray scattering (SAXS) was much less than 0.1 μm [26].

The fresh catalyst was crushed and sieved to 0.25–0.36 mm (40–60 ASTM mesh) in size. The weight of the catalyst loaded was 4.75 g. The catalyst was diluted using quartz sand with the same mesh size range. The volume ratio of catalyst to quartz sand was 1:6.

The catalyst was reduced in situ using syngas with H_2/CO = 1.0, at 553 K, 0.15–0.20 MPa, 1800 rpm and space velocity of 0.23×10^{-3} N m^3 kg_{cat}^{-1} s^{-1} for 48 h. Then, the reaction temperature was programmed to 493 K, and the operation conditions were adjusted to the desired values for the Fischer-Tropsch synthesis. The reactor stirring speed of all the experiments were carried out at 1800 rpm, which is safe to eliminate the external mass transfer limitations [27].

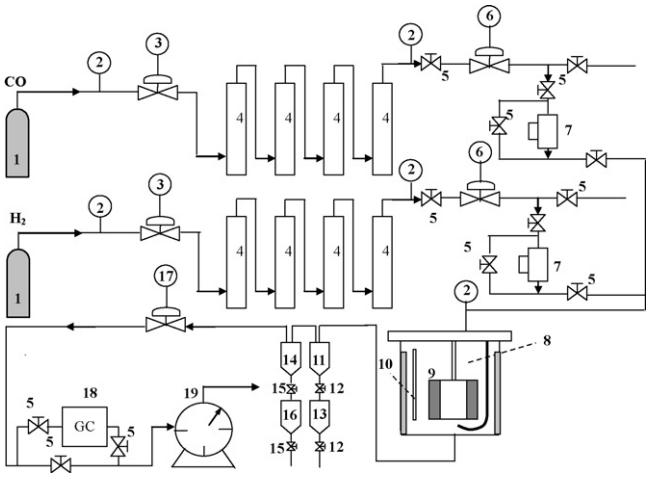

Fig. 1. Experimental set-up: (1) gas cylinders; (2) pressure gauges; (3) pressure regulators; (4) purification columns; (5) needle valves; (6) pressure regulators before the reactor; (7) mass flow controllers; (8) reaction tank; (9) basket reactor; (10) thermowell; (11) wax condenser; (12) high temperature ball valves; (13) wax trap (hot trap); (14) oil/water condenser; (15) ball valves; (16) cold trap; (17) back pressure regulator; (18) on-line GC analysis; (19) wet flow meter.

2.2. Reactor system

The continuous spinning basket reactor (stainless steel, $H = 0.081$ m, $D_0 = 0.052$ m, $D_i = 0.046$ m) system is shown in Fig. 1. A detailed description of the reactor has been provided elsewhere [27]. Before entering the reactor, the CO (>99.99%) and H_2 (>99.95%) streams passed through a series of columns for removing tiny amounts of oxygen, sulfur, carbonyls and water. The flow rates of the feed gases were controlled by using two Brooks 5850E mass flow meters. The outlet of the reactor was connected to a hot trap (393 K) and then an ice trap (273 K). After these product collectors, the tail gas was measured by a wet gas flow meter.

2.3. Operating procedure

Blank experiments with quartz sand instead of the Fe-Mn catalyst had been firstly carried out under the same conditions as the normal experiments. This showed that the silica sand has no activity for the conversion of synthesis gas.

A series of experiments were carried out under a wide range of reaction conditions. Before collecting experimental data, the system was allowed to run undisturbed for 100 h to reach steady state. After the conclusion of this unsteady-state period, the variables were adjusted to the required operational parameters. Liquid samples were collected in the hot trap and ice trap over 12 h periods (mass balance period), and the exit tail gas composition and its flow rate were measured at least three times during the mass balance period. After a mass balance period, a steady-state run was performed for more than 10 h, and the next

sampling period was carried out. The total mass balance in the system was kept at the level of 95–103%.

2.4. Product analysis

The purified syngas and the tail gas were analyzed on-line using a gas chromatograph (Agilent 6890N). H_2, O_2, N_2, CH_4 and CO were separated on MoleSieve 5A capillary column (30 m × 530 μm i.d., Ar carrier flow) and detected with a thermal conductivity detector (TCD). C_1–C_8 hydrocarbons in the gas phase were analyzed on HP-PLOT Al_2O_3 capillary column (50 m × 530 μm i.d.) with a flame ionization detector (FID) and N_2 carrier. CO_2 in the tail gas was measured periodically on-line using an Agilent 4890D GC equipped with TCD (H_2 carrier) and quantified using the external standard method. The oil product from the cold trap was analyzed using a GC with a DB-1 capillary column (60 m × 320 μm i.d. FID, N_2 carrier). The temperature was raised from 333 K (maintained for 16 min) to 563 K at the rate of 3 K/min. The wax product from the hot trap was firstly dissolved in CS_2 (0.5–1.0 mass%) and then analyzed using an Agilent 6890N GC with OV-101 capillary column (FID, N_2 carrier) with temperature programming (2 K/min) from 323 to 573 K. Oxygenate products dissolved in water were measured by an Agilent 6890N GC with DB-WAX capillary column (FID, N_2 carrier).

3. Results and discussion

The effects of reaction temperature, total pressure, space velocity and H_2/CO ratio on the catalytic performance of the Fe-Mn catalyst are summarized in Tables 1–4. The experimental process in the spinning basket reactor was as follows: the reaction temperature increased from 533 to 553 K firstly, and then at 553 K we kept the total pressure constant at 1.49 MPa and varied the space velocity. After that, when temperature increased to 563 K, we kept the space velocity at 0.93×10^{-3} N m^3 kg$_{cat}^{-1}$ s^{-1} and varied the reaction pressure. Subsequently, when temperature increased to 573 K we kept the space velocity at 1.39×10^{-3} N m^3 kg$_{cat}^{-1}$ s^{-1} and varied the H_2/CO ratio.

3.1. Effect of reaction temperature

In Table 1 (columns 1, 2, 6 and 10), it can be seen that with increasing temperature from 533 to 563 K, the CO conversion gradually increased from 44.86% to 59.54%. It seems that increasing temperature has little influence on CO_2 selectivity, which remains at about 45% in the temperature range of 533–563 K. With increasing temperature, the H_2/CO usage ratio decreased slightly from 0.69 to 0.66.

The methane selectivity increased with increasing temperature. It is owing to the increased H_2/CO ratio inside the reactor. From Table 1, it can also be seen that the selectivity to light alkenes is relatively high, and increased with increasing temperature except for ethylene, which decreased from 4.53% to 3.50%. Bukur et al. [28] investigated a precipitated iron catalyst (100Fe/5Cu/4.2K/25SiO_2 on mass basis) in a fixed bed reactor under a variety of process conditions, and have also observed that ethylene selectivity was the highest at the lowest reaction temperature during supercritical FTS at a nearly constant syngas conversion (∼30%).

It is generally assumed, that the olefin readsorption probability increases with increasing carbon number due to increased residence times of longer chains in the liquid-filled pores of

Table 1
Effect of reaction conditions on catalytic performance in spinning basket reactor (H_2/CO = 1.00 in feed gas)

Temperature (K)	533	543	553	553	553	553	553	553	563	563	563	563
Pressure (MPa)	1.49	1.49	1.49	1.49	1.49	1.49	1.49	1.49	0.93	1.49	1.96	2.53
Space velocity ($\times 10^{-3}$ N m^3 kg$_{cat}^{-1}$ s^{-1})	0.93	0.93	0.46	0.58	0.69	0.93	1.39	1.85	0.93	0.93	0.93	0.93
Time on stream (h)	117	265	338	360	384	408	432	456	480	504	528	552
CO conversion (%)	44.86	53.02	81.81	73.58	66.48	54.74	37.98	29.85	42.95	59.54	70.97	75.01
CO_2 selectivity (%)	44.98	48.81	45.39	45.18	43.77	44.03	45.60	45.18	45.38	45.09	43.82	43.95
H_2/CO in tail gas	1.25	1.37	2.56	2.03	1.70	1.41	1.19	1.11	1.28	1.51	1.78	1.96
H_2/CO usage ratio	0.69	0.67	0.66	0.64	0.66	0.66	0.70	0.72	0.63	0.66	0.68	0.68
Hydrocarbon selectivity (wt%)												
CH_4	5.06	6.83	11.05	11.08	10.07	9.71	8.92	8.24	11.16	11.41	12.17	11.41
$C_2^=$	4.53	3.71	2.22	2.67	2.91	3.72	4.70	5.11	4.68	3.50	3.11	2.98
C_2^0	1.91	3.89	8.59	8.29	7.03	6.09	4.72	3.85	6.10	6.98	8.01	8.17
$C_3^=$	7.18	8.85	10.74	11.35	10.76	11.09	10.92	10.40	11.92	11.80	12.30	11.92
C_3^0	1.26	1.74	4.84	4.38	3.42	2.72	2.09	1.78	2.47	3.21	3.93	4.13
$C_4^=$	5.02	6.22	7.70	8.18	7.62	7.81	7.85	7.47	8.62	8.34	8.14	7.30
C_4^0	1.09	1.38	2.57	2.52	2.13	1.90	1.65	1.47	1.71	2.05	2.26	2.18
C_5^+	73.95	67.38	52.29	51.53	56.06	56.96	59.15	61.68	53.34	52.71	50.08	51.92
$C_{2-4}^=/C_{2-4}^0$ (mol/mol)	3.80	2.35	1.07	1.22	1.42	1.80	2.43	2.90	2.09	1.63	1.39	1.29
CO conversion rate (mol kg$_{cat}^{-1}$ s^{-1})	0.93	1.09	0.84	0.95	1.03	1.13	1.18	1.23	0.89	1.23	1.46	1.55
CO_2 formation rate (mol kg$_{cat}^{-1}$ s^{-1})	0.42	0.53	0.38	0.43	0.45	0.50	0.54	0.56	0.40	0.55	0.64	0.68
FTS reaction rate (mol kg$_{cat}^{-1}$ s^{-1})	0.51	0.56	0.46	0.52	0.58	0.63	0.64	0.68	0.48	0.68	0.82	0.87
Oxygenates formation rate ($\times 10^{-3}$ g kg$_{cat}^{-1}$ s^{-1})	5.33	6.31	3.09	3.83	4.29	6.94	8.02	6.76	4.55	7.84	9.69	11.39

Table 2
Effect of reaction temperature on the WGS reaction and the selectivity to oxygenates

	Temperature (K)			
	533	543	553	563
The water formation rate ($\times 10^{-3}$ g kg_{cat}^{-1} s^{-1})	26.08	20.60	18.17	17.30
Oxygenates in water (wt%)	16.44	19.71	22.03	22.96
Oxygenates in oil (wt%)	22.47	20.48	13.68	15.23
Acids/oxygenates in water (wt%)[a]	21.40	11.42	4.21	4.58
Alcohols/oxygenates in water (wt%)[b]	69.49	79.01	88.48	87.17
Alcohols in total oxygenates (wt%)[c]	72.72	80.01	77.97	74.67
Acids in total oxygenates (wt%)	18.64	9.49	10.78	12.17
Ketones in total oxygenates (wt%)	4.41	5.25	4.46	4.33
Aldehydes in total oxygenates (wt%)	4.23	5.25	6.79	8.82
Q_p ($P_{CO_2} P_{H_2}$)/($P_{CO} P_{H_2O}$)	3.56	6.32	6.84	8.56
K_p, equilibrium constant of WGS reaction	73.19	62.10	53.02	45.54

Reaction conditions: $P = 1.49$ MPa, $H_2/CO = 1.00$, space velocity = 0.93×10^{-3} N m^3 kg_{cat}^{-1} s^{-1}.
[a] Acids in oxygenates of water phase.
[b] Alcohols in oxygenates of water phase.
[c] Total oxygenates denotes that the total oxygenate products of both oil and water phases.

the catalyst. Schulz and Gokcebay [29] mentioned secondary hydrogenation as the most important process for the selectivity to the FTS products on iron catalysts promoted with one of the transition metals Mn, Ti, Cr, Zr or V. To obtain more insight into the role of secondary olefin reactions during FTS and the reason for their chain length dependence, Schulz and Claeys [30] have extensively studied on the extent and selectivity of olefin reactions at different reaction conditions (variation of CO partial pressure and reaction temperature), with cobalt catalysts and particular emphasis on the chain length dependence of secondary olefin reactions by co-feeding α-olefins (C_2–C_{11}) during FTS reaction in a gradientless slurry reactor. They proposed that the chain length dependencies of individual reaction pathways are in agreement with the selectivities observed in the base case experiments and mainly due to carbon number dependent solubility of the olefins in the liquid reaction product.

There is general agreement that ethylene is much more reactive than propylene or butylene, therefore with the outlet H_2/CO ratio increased a little from 1.25 to 1.51, ethylene readsorption and secondary hydrogenation reaction are much stronger than that of propylene and butylene, as ethylene is one of the most active species in the complicated FTS reactions. Hence, the ethylene selectivity decreased with the increasing reaction tem-

Table 3
Effect of H_2/CO ratio on the catalytic performance

	In spinning basket reactor (SBR)					In fixed bed reactor (FBR)			
	0.80[a]	1.21[a]	1.61[a]	1.98[a]	2.50[a]	0.80[a]	1.00[a]	1.50[a]	2.00[a]
Time on stream h)	600	625	648	673	697	757	783	842	866
CO conversion (%)	50.66	61.45	72.16	79.17	82.73	64.63	74.12	81.12	88.32
CO_2 selectivity (%)	47.19	44.12	41.34	37.93	34.90	47.47	44.84	40.62	41.55
H_2/CO molar ratio in tail gas	0.98	1.95	3.62	6.05	9.58	1.08	1.80	4.14	9.59
H_2/CO molar usage ratio	0.63	0.74	0.84	0.91	1.02	0.64	0.73	0.88	0.99
Hydrocarbon selectivity (wt%)									
CH_4	8.14	12.14	16.06	16.98	19.66	5.99	6.74	9.25	11.23
$C_2^=$	4.59	3.88	3.90	3.84	3.91	4.06	4.36	5.18	5.32
C_2^0	4.76	7.49	9.94	10.48	11.83	1.18	1.86	3.26	4.18
$C_3^=$	11.09	12.42	13.68	13.34	13.68	5.58	6.91	9.22	10.23
C_3^0	2.00	3.48	4.79	5.07	5.77	0.80	1.84	3.09	3.47
$C_4^=$	7.62	8.56	8.85	8.47	8.67	4.22	6.20	6.64	8.75
C_4^0	1.41	2.18	2.67	2.77	3.11	0.70	0.99	1.61	1.86
C_5^+	60.41	49.85	40.11	39.06	33.38	77.47	71.10	61.75	54.96
$C_{2-4}^=/C_{2-4}^0$ (mol/mol)	2.47	1.60	1.28	1.18	1.07	5.17	3.72	2.64	2.56
CO conversion rate (mol kg_{cat}^{-1} s^{-1})	1.74	1.72	1.71	1.64	1.46	2.07	2.12	1.87	1.69
CO_2 formation rate (mol kg_{cat}^{-1} s^{-1})	0.82	0.76	0.71	0.62	0.51	0.98	0.95	0.76	0.70
FTS reaction rate (mol kg_{cat}^{-1} s^{-1})	0.92	0.96	1.00	1.02	0.95	1.09	1.17	1.11	0.99
Oxygenates formation rate ($\times 10^{-3}$ g kg_{cat}^{-1} s^{-1})	14.54	16.74	16.21	15.39	16.76	12.69	12.19	14.18	14.59

Reaction conditions: $T = 573$ K, $P = 2.02$ MPa, SV = 1.39×10^{-3} N m^3 kg_{cat}^{-1} s^{-1} (SBR); 1.29×10^{-3} N m^3 kg_{cat}^{-1} s^{-1} (FBR).
[a] H_2/CO molar ratio in feed gas.

Table 4
Effect of H_2/CO ratio on the WGS reaction and the selectivity to oxygenates

	H_2/CO ratio in feed gas				
	0.80	1.21	1.61	1.98	2.50
The water formation rate ($\times 10^{-3}$ g kg_{cat}^{-1} s^{-1})	21.99	38.57	54.13	59.81	69.67
Oxygenates in water (wt%)	27.18	24.12	20.21	17.56	18.89
Oxygenates in oil (wt%)	20.71	17.28	15.46	14.64	14.44
Acids/oxygenates in water (wt%)[a]	6.64	4.69	4.05	4.10	2.91
Alcohols/oxygenates in water (wt%)[b]	81.22	83.34	85.39	88.08	88.27
Alcohols in total oxygenates (wt%)[c]	71.43	74.99	79.50	81.34	83.48
Acids in total oxygenates (wt%)	12.44	10.32	7.57	6.69	5.21
Ketones in total oxygenates (wt%)	4.29	6.31	5.80	5.37	4.94
Aldehydes in total oxygenates (wt%)	11.85	8.38	7.12	6.60	6.38
Q_p ($P_{CO_2} P_{H_2}$)/($P_{CO} P_{H_2O}$)	6.51	6.87	8.46	11.31	12.60

Reaction conditions: $T = 573$ K, $P = 2.02$ MPa, SV = 1.39×10^{-3} N m^3 kg_{cat}^{-1} s^{-1}.
[a] Acids in oxygenates of water phase.
[b] Alcohols in oxygenates of water phase.
[c] Total oxygenates denotes that the total oxygenate products of both oil and water phases.

perature under these reaction conditions in the spinning basket reactor.

From the results, it can also be concluded that higher temperature is preferential for chain termination to produce light hydrocarbons, while lower temperature is preferential for chain growth and the production of heavy hydrocarbons [31].

The $C_{2-4}^{=}/C_{2-4}^{0}$ ratio decreased from 3.80 to 1.63 with increasing temperature due to the decreased ethylene and increased ethane from 1.91% to 6.98%. Similar results were reported by Donnelly and Satterfield [32], Bukur and Patel [33] and Van der Laan [34]. Low hydrogen concentrations in the feed and in the reactor result in the low hydrogen surface concentrations and promote the termination to olefins instead of saturated paraffins [34].

It is well known that the chemical reaction rate as one of the most important parameters plays a significant role in scale-up a FT reactor and industrial design. The effects of reaction conditions on the reaction rates are also shown in Table 1. The CO conversion rate, CO_2 formation rate and FTS reaction rate all increased with increasing reaction temperature from 533 to 563 K. The FTS reaction rate basically increased linear with increasing temperature, as shown in Fig. 2a. Similar results were also obtained by Schulz and Claeys [30,35]. From the reactions of added olefins (assuming that their FTS formation rates were not affected by olefin addition), they also confirmed that olefins were preferentially consumed via secondary reactions at high reaction temperatures [30]. Both the CO conversion rate and CO_2 formation rate followed the same trends as the FTS reaction rate, and almost presented a linear correlation with increasing reaction temperature.

The oxygen-containing products of FTS have received much more attention since the pioneering work of Emmett and co-workers [36–41]. Though the content of the oxygenates is small relative to the total products, it has significant influence on the upgrading of primary FTS products. Therefore, discussing the selectivity to oxygenates in total products is important. It may also provide some valuable information for understanding the complex FTS reaction mechanism from the point of view of conservation of mass.

The overall oxygenates formation rate is listed in Table 1. With increasing temperature from 533 to 563 K, the overall oxygenates formation rate increased from 5.33×10^{-3} to 7.84×10^{-3} g kg_{cat}^{-1} s^{-1}. The detailed information regarding different oxygenate species is given in Table 2. It shows that with increasing temperature, the water formation rate decreased from 26.08×10^{-3} to 17.30×10^{-3} g kg_{cat}^{-1} s^{-1}. The selectivity to oxygenates in water increased from 16.44% to 22.96%, while the selectivity to oxygenates in oil decreased from 22.47% to 15.23%. However, as mentioned above the overall oxygenates formation rate increased with the increase of reaction temperature.

The acids and alcohols with lower molecular weight are mainly dissolved in water, while alcohols with higher molecular weight are mainly dissolved in oil, and oxygenates in wax are usually negligible. From Table 2, it can also be seen that oxygenates are mainly alcohols with small amounts of acids, ketones and aldehydes. For water phase, the selectivity to acids in oxygenates decreased sharply from 21.40% to 4.58%, while the selectivity to alcohols in oxygenates increased from 69.49% to 87.17% with increasing reaction temperature. The selectivities to alcohols, acids, ketones and aldehydes in total oxygenates are summarized, respectively, in Table 2. The increased reaction temperature seems to have little effect on the selectivity to ketones, while aldehydes in total oxygenates increased, as can be seen in Table 2. Due to the complexity of the reaction mechanism for the formation of oxygenates, it should be studied further from other aspects.

Here, we define the experimental $P_{CO_2} P_{H_2} / P_{CO} P_{H_2O}$ value as Q_p (for the indication of the extent of water gas shift (WGS) reaction), which increases from 3.56 to 8.56 with increasing reaction temperature from 533 to 563 K, and the Q_p values are far lower than the K_p (equilibrium constant of WGS reaction), which decreases from 73.19 to 45.54. This indicates that the WGS reaction is far from equilibrium under these reaction con-

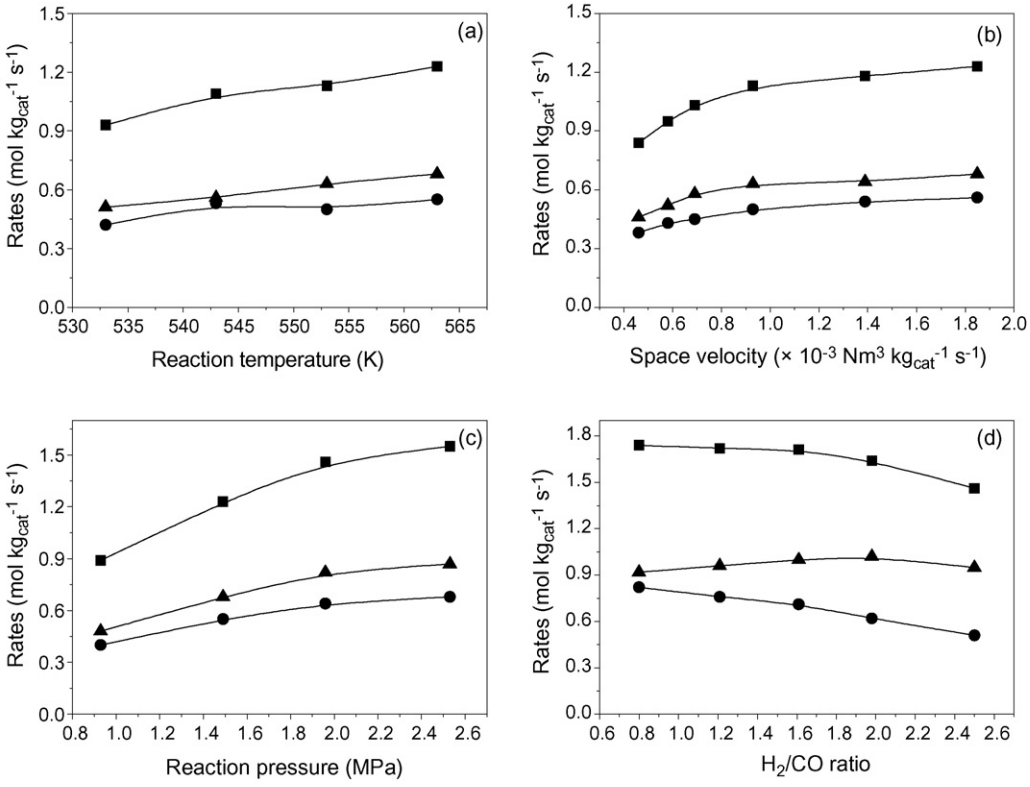

Fig. 2. Effect of reaction conditions on the reaction rates in the spinning basket reactor (reaction conditions are shown in Tables 1 and 3): (■) CO conversion rate; (▲) FTS reaction rate; (♦) CO_2 formation rate.

ditions, and this phenomenon has also been observed by others [25,42].

3.2. Effect of space velocity

Table 1 also shows the effect of space velocity on the catalytic performance at 553 K. The CO conversion decreased sharply from 81.81% to 29.85% with increasing space velocity from 0.46×10^{-3} to 1.85×10^{-3} N m^3 kg$_{cat}^{-1}$ s^{-1}, while the space velocity has little effect on the CO_2 selectivity, which remains at about 45%. Increasing space velocity can decrease residence time of reactants and products, which leads to a decrease in CO conversion.

The selectivities to methane, ethane, propane and butane gradually decreased, while the selectivity to ethylene increased and the selectivities to propylene and butylene have no apparent change. The selectivity to C_5^+ increased in mass with increasing space velocity. The effect of space velocity on the hydrocarbon selectivity is relatively complex. On one hand, higher space velocity shortens the residence time, which is unfavorable for chain growth. On the other hand, the lower H_2/CO ratio in the reactor is favorable for the chain growth. As a result, under different reaction conditions, the various space velocities can lead to different results. In this reaction, the effect of space velocity on the H_2/CO ratio is remarkable, and in turn the lower H_2/CO ratio in the reactor results in a higher C_5^+ selectivity.

Consistent with our previous findings, ethylene shows unique behavior, namely, the selectivity to ethylene increased with increasing space velocity, which was contrary to other low molecular weight hydrocarbons. The same trend was also observed by Van der Laan [34] on a commercial Fe-Cu-K-SiO_2 catalyst in a continuous spinning basket reactor and Bukur et al. [28] on a commercial Ruhrchemie catalyst in a fixed bed reactor. Madon et al. [43] studied the effect of space velocity on the selectivity to olefins and paraffins on Ru catalyst, and found that the olefin selectivities increased with increasing space velocity.

The $C_{2-4}^{=}/C_{2-4}^{0}$ ratio increased from 1.07 to 2.90 with increasing space velocity as shown in Table 1. With the increase of space velocity, the FTS reaction rate increased visibly at first, subsequently, with the space velocity increased further, a more gradual increase of FTS reaction rate was observed, as can be seen from Fig. 2b. The CO conversion rate and CO_2 formation rate have the similar trends as the FTS reaction rate. The overall oxygenates formation rate increased from 3.09 to 8.02×10^{-3} g kg$_{cat}^{-1}$ s^{-1} with increasing space velocity from 0.46 to 1.39×10^{-3} N m^3 kg$_{cat}^{-1}$ s^{-1}. However, when the space velocity increased further, the overall oxygenates formation rate decreased to some extent.

3.3. Effect of reaction pressure

In commercial process, the FTS reaction usually operates under high pressure. The effect of reaction pressure on the catalytic performance is shown in Table 1. The CO conversion increased from 42.95% to 75.01% with increasing pressure from 0.93 to 2.53 MPa. This is due to the enhanced concentration of

active surface carbon species with increasing pressure and the improved collision probability of the catalysts and reactants. Thus, the rate of reaction is enhanced.

As shown in Table 1, increasing the pressure has little influence on the hydrocarbon selectivities. The selectivity to low carbon number alkanes increased slightly, while the selectivities to ethylene and butylene decreased a little, and the propylene selectivity did not vary much. The increased selectivity to low carbon number alkanes may be attributed to the increased H_2/CO ratio in tail gas, which is favorable for the hydrogenation reaction. And as we mentioned above, the appreciable increase in tail gas H_2/CO ratio with increasing reaction pressure also promotes the readsorption and secondary reactions of ethylene much more than other species. Thus, the selectivity to ethylene decreased with increasing pressure. However, the selectivities to C_3, C_4 and C_5 olefins are only slightly affected by secondary hydrogenation [29]. Therefore, the reaction pressure has little effect on them. As a whole, increasing pressure enhances hydrogenation to some extent, and results in the decrease of $C^{=}_{2-4}/C^{0}_{2-4}$ ratio from 2.09 to 1.29.

As displayed in Fig. 2c, the FTS reaction rate, CO conversion rate and CO_2 formation rate followed the similar trends as that of Fig. 2b. Therefore, it indicated that choosing the optimum space velocity and pressure under certain reaction temperature and H_2/CO ratio can utilize the raw material farthest and gain the products maximum. The overall oxygenates formation rate also increased from 4.55×10^{-3} to 11.39×10^{-3} g kg_{cat}^{-1} s^{-1} with increasing pressure from 0.93 to 2.53 MPa.

3.4. Effect of H_2/CO ratio

As mentioned above, the H_2/CO ratio plays an important role in the FTS reaction. The effect of H_2/CO ratio on catalytic performance in the stirred basket reactor is shown in Table 3, and compared with that in the fixed bed reactor under the similar reaction conditions.

As shown in Table 3, CO conversion increased with increasing H_2/CO ratio in both reactors. The CO_2 selectivity decreased with increasing H_2/CO ratio due to the increase of the hydrogen partial pressure and the weakened force of the positive water gas shift reaction. And H_2/CO usage ratio also increased with increasing H_2/CO ratio in feed gas.

It can be found from Table 3 that the selectivity to light hydrocarbons increased with increasing H_2/CO ratio in both reactors except for ethylene in the spinning basket reactor. Under these reaction conditions, ethylene again showed its unique character compared with other product species. This phenomenon is very interesting and should be studied further from other aspects. From a comparison of the methane selectivity in the two reactors, it can be found that the methane selectivity in the spinning basket reactor is higher than that in the fixed bed reactor despite the higher space velocity.

The quantitatively description of FTS product distribution mathematically as a polymerization reaction, generally believed to form stepwise by insertion or addition of C_1 intermediates with constant growth probability, is given by the Anderson–Schulz–Flory (ASF) distribution [44,45], and may be presented as:

$$\frac{W_n}{n} = (1-\alpha)^2\alpha^{n-1} \quad (1)$$

where W_n is the weight fraction of the products with n carbon number and α is the chain growth probability or growth factor. The logarithmic form of this kinetic expression is shown below:

$$\log\left(\frac{W_n}{n}\right) = \log(\ln^2\alpha) + n\log\,\alpha \quad (2)$$

According to the equation, a plot of $\log(W_n/n)$ versus n should given a straight line (ASF plot) and the chain growth probability α can be calculated from the slope of the ASF distribution.

The results reported in Fig. 3 show the changes observed in the detailed product distributions when the H_2/CO ratio was increased from 0.80 to 2.50 in the spinning basket reactor at 573 K. The product distributions are discussed by using the plot of $W_n/n \sim n$, and the deviations from the simple ASF distributions have been observed. From the results, it can also draw the conclusions that the higher H_2/CO ratio is preferential for chain termination to produce light hydrocarbons while lower H_2/CO ratio is preferential for the chain growth and the production of heavy hydrocarbons [31,46,47]. Therefore, the C_5^+ selectivity decreased with increasing H_2/CO ratio.

The curve at low H_2/CO ratio of 0.80 in Fig. 3 seems to indicate α-olefin readsorption on the growth sites, as favored by low secondary olefin hydrogenation and isomerization, high wax yield and long residence time. In order to explain, the main deviations of hydrocarbon distribution from the ASF law, namely the increase of the chain growth factor with the increase of carbon number, the olefin readsorption and secondary reactions were involved in the kinetics and reactor models [34,48–51]. Schluz and Claeys [48] extended their existing kinetic model taking into account olefin hydrogenation, isomerization (double bond shift) and incorporation and in particular chain length dependent product solubilities, and typical deviations from ideal distribu-

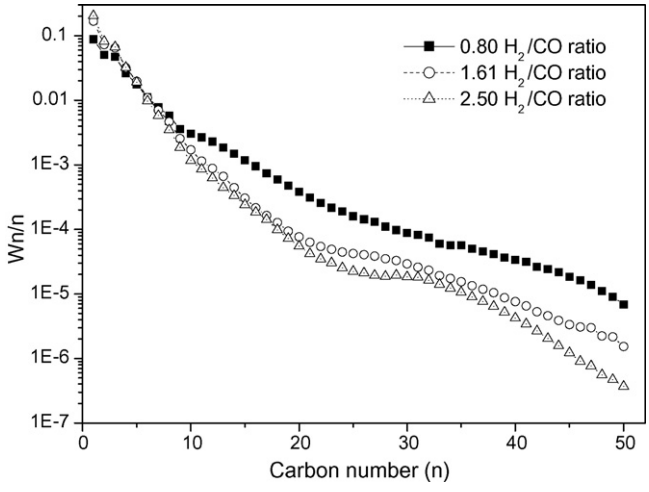

Fig. 3. Effect of H_2/CO ratio on the distribution of hydrocarbon with different carbon number in the spinning basket reactor. Reaction conditions: $T = 573$ K, $P = 2.02$ MPa, SV = 1.39×10^{-3} N m^3 kg_{cat}^{-1} s^{-1}.

tions can be simulated and experimentally observed data can be satisfactorily described.

The enhanced hydrogenation resulting from increasing the H_2/CO ratio leads to a decrease of $C^{=}_{2-4}/C^{0}_{2-4}$ ratio. The CO conversion rate and CO_2 formation rate decreased with increasing H_2/CO ratio, while the FTS reaction rate increased slightly and then decreased a little when the H_2/CO ratio equal to 2.50. The similar trends were also observed in the fixed bed reactor. The overall oxygenates formation rate increased slightly with increasing H_2/CO ratio as a whole.

It is well known that the H_2/CO ratio in the reaction atmosphere plays a very important role in FTS reactions, and influences the product selectivity directly. Moreover, the liquid products from the FTS process may contain a relatively large amount of oxygenates. These oxygenates normally consist of various functional groups (alcohols, ketones, esters, carboxylic acids, aldehydes) and may be present over a wide carbon number range, e.g. C_1–C_{40} [52]. Since the total amount of oxygenates in FTS products over iron-based catalysts is higher relative to that of cobalt-based catalysts [53], it is necessary to discuss the selectivity to oxygenates at different H_2/CO ratios in the spinning basket reactor. With H_2/CO ratio increasing from 0.80 to 1.61, the water formation rate significantly increased from 21.99×10^{-3} to 69.67×10^{-3} g kg_{cat}^{-1} s^{-1}, as presented in Table 4. The selectivities to oxygenates in water and oil decrease from 27.18% to 20.21% and from 20.71% to 15.46%, respectively. However, with the H_2/CO ratio being enhanced further, the influence on the proportion of oxygenates in water and oil is not clear. This shows that the proper H_2/CO ratio in feed gas can result in gaining the optimal selectivities to light olefins and high-quality fuels. From Table 4, it can also be seen that the selectivity to acids in oxygenates for water phase decreased from 6.64% to 2.91% while the selectivity to alcohols in oxygenates for water phase increased from 81.22% to 88.27% with increasing the H_2/CO ratio. This indicates that the increased H_2/CO ratio favors alcohol formation and hinders the formation of acids. These conclusions can be summarized as follows: alcohols in total oxygenates monotonically increased from 71.43% to 83.48%, while acids in total oxygenates decreased monotonically from 12.44% to 5.21%. The increased H_2/CO ratio seems to have little effect on the selectivity to ketones in total oxygenates which does not change too much. The aldehydes in total oxygenates decreased from 11.85% to 6.38% with increasing H_2/CO ratio. From Table 4, it can be seen that the Q_p values increased monotonically from 6.51 to 12.60. This may be attributed to the increased partial pressure of H_2 due to the increasing H_2/CO ratio. But the Q_p values are still lower than the equilibrium value K_p, which is 39.33 at 573 K.

The detailed product distribution of oxygenates under different H_2/CO ratios is illustrated in Fig. 4. It is found that the oxygenate distribution is similar to the hydrocarbon distribution except for the C_1 oxygenates. The distribution of low molecular weight oxygenates increased with increasing H_2/CO ratio, while when carbon number exceeds 4, the distribution of oxygenates decreased with increasing H_2/CO ratio. This phenomenon is in accord with the distributions of hydrocarbons. From these results, it can also be concluded that a higher H_2/CO ratio is preferential for chain termination to produce light oxygenates products while a lower H_2/CO ratio is preferential for chain growth and the formation of heavy oxygenate products. The FTS products follow the ASF distribution, which is characterized either by a single value or by two values of the chain growth probability factor (Anderson [44], Huff and Satterfield [54]) [55]. The product distribution of oxygenates seems to obey the rule of ASF distribution except for the C_1 oxygenates. In fact, methanol is the mainly component in C_1 oxygenates. From Fig. 4, it can also be seen that C_2 oxygenates (mainly comprised of ethanol) are the principal components. When the carbon number is greater than 10, the proportion of oxygenates is becoming smaller, and may be neglected. Although the proportion of oxygenates is relatively small, some studies clearly showed that alcohols could serve as chain initiators for the polymerization reactions [36,37,41], and acids in small amounts can corrode the equipment which may contribute to direct economic loss in a commercial process. Since oxygenates play such an important role in mechanistic considerations for the FTS reaction, a further investigation into the distribution of oxygenates should be considered.

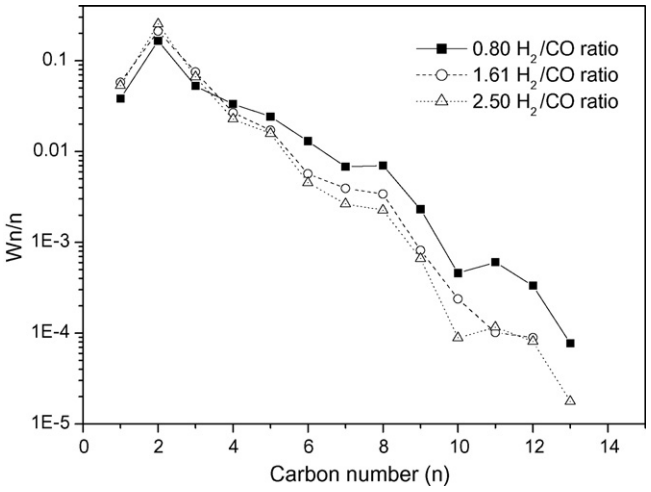

Fig. 4. Effect of H_2/CO ratio on the distribution of oxygenates with different carbon number in the spinning basket reactor. Reaction conditions: $T = 573$ K, $P = 2.02$ MPa, SV = 1.39×10^{-3} N m^3 kg_{cat}^{-1} s^{-1}.

4. Conclusions

The effects of reaction conditions including temperature, total pressure, space velocity, and synthesis gas composition on the FTS performance over an Fe-Mn catalyst have been carried out in a continuous spinning basket reactor. The catalyst showed a relatively stable activity during a run of about 700 h. The Fe-Mn catalyst presented a higher activity towards the formation of hydrocarbons, especially the formation of lower molecular weight alkenes.

The reaction conditions strongly influenced the performance of the catalyst, and the product selectivities are changed markedly with the variation of H_2/CO ratio in reaction atmosphere, particularly for that of alkenes. In this work, ethylene shows unique selectivity owing to the fact that ethylene is more

reactive than other low molecular weight α-olefins. The selectivity to ethylene decreased with increasing reaction temperature, pressure and inlet H_2/CO ratio, and increased with the increase of space velocity, which is contrary to the behavior of other low molecular weight hydrocarbons. The high hydrogen partial pressure can enhance the hydrogenation and restrain the growth of carbon chains. Hence, choosing a suitable inlet H_2/CO ratio can result in optimal catalytic performance of the catalyst, and achieve the optimal production of light olefins and high quality liquid fuels to meet the continuously increasing demands for liquid fuels and chemical raw materials.

The FTS reaction rate and the overall oxygenates formation rate generally increased with increasing reaction temperature, pressure, space velocity and H_2/CO ratio.

Increasing reaction temperature can markedly decrease the selectivity to acids in oxygenates for water phase. Increasing the inlet H_2/CO ratio at 573 K can also decrease the selectivity to acids, which is much lower than at low temperatures. Alcohols (especially ethanol) are the main components in total oxygenates. The carbon distribution of oxygenates follows the ASF distribution except for the C_1 oxygenates.

Acknowledgments

Financial support from the National Outstanding Young Scientists Foundation of China (Project No. 20625620) and National Natural Science Foundation of China (Project No. 20590361) are gratefully acknowledged. This work is also supported by Synfuels CHINA Co., Ltd.

References

[1] M.E. Dry, Appl. Catal. A 189 (1999) 185.
[2] H. Schulz, Appl. Catal. A 186 (1999) 3.
[3] J.R. Rostrup-Nielsen, Catal. Rev. Sci. Eng. 46 (2004) 247.
[4] S. Li, G.D. Meitzner, E. Iglesia, J. Phys. Chem. B 105 (2001) 5743.
[5] G.P. Van der Laan, A.A.C.M. Beenackers, Catal. Rev. Sci. Eng. 41 (1999) 255.
[6] G.C. Maiti, R. Malessa, M. Baerns, Appl. Catal. 5 (1983) 151.
[7] G.C. Maiti, R. Malessa, U. Löchner, H. Papp, M. Baerns, Appl. Catal. 16 (1985) 215.
[8] K.M. Kreitman, M. Baerns, J.B. Butt, J. Catal. 105 (1987) 319.
[9] Y. Yang, H.W. Xiang, R.L. Zhang, B. Zhong, Y.W. Li, Catal. Today 106 (2005) 170.
[10] Y. Yang, H.W. Xiang, L. Tian, H. Wang, C.H. Zhang, Z.C. Tao, Y.Y. Xu, B. Zhong, Y.W. Li, Appl. Catal. A 284 (2005) 105.
[11] T. Herranz, S. Rojas, F.J. Pérez-Alonso, M. Ojeda, P. Terreros, J.L.G. Fierro, Appl. Catal. A 311 (2006) 66.
[12] C.H. Zhang, Y. Yang, B.T. Teng, T.Z. Li, H.Y. Zheng, H.W. Xiang, Y.W. Li, J. Catal. 237 (2006) 405.
[13] B. Büssemeier, Hydrocarbon Process. 55 (1976) 105.
[14] H. Kölbel, K.D. Tillmetz, US Patent 4,177,203 (1979).
[15] J. Barrault, C. Forquy, V. Perrichon, Appl. Catal. 5 (1983) 119.
[16] H.W. Pennline, M.F. Zarochak, R.E. Tischer, R.R. Schehl, Appl. Catal. 21 (1986) 313.
[17] N.K. Jaggi, L.H. Schwartz, J.B. Butt, H. Popp, M. Baerns, Appl. Catal. 13 (1985) 347.
[18] K.B. Jensen, F.E. Massoth, J. Catal. 92 (1985) 98.
[19] K.B. Jensen, F.E. Massoth, J. Catal. 92 (1985) 109.
[20] U. Löchner, H. Papp, M. Baerns, Appl. Catal. 23 (1986) 339.
[21] R. Malessa, M. Baerns, Ind. Eng. Chem. Res. 27 (1988) 279.
[22] W.L. van Dilk, J.W. Niemantsverdriet, A.M. van der Kraan, H.S. van der Baan, Appl. Catal. 2 (1982) 273.
[23] B. Zhong, Q. Wang, S.Y. Peng, Chinese Patent ZL 95/106 156.9 (1995).
[24] Y.Y. Ji, H.W. Xiang, J.L. Yang, Y.Y. Xu, Y.W. Li, B. Zhong, Appl. Catal. A 214 (2001) 77.
[25] L. Bai, H.W. Xiang, Y.W. Li, Y.Z. Han, B. Zhong, Fuel 81 (2002) 1577.
[26] X.G. Li, B. Zhong, S.Y. Peng, Q. Wang, Catal. Lett. 23 (1994) 245.
[27] B.T. Teng, J. Chang, J. Yang, G. Wang, C.H. Zhang, Y.Y. Xu, H.W. Xiang, Y.W. Li, Fuel 84 (2005) 917.
[28] D.B. Bukur, X. Lang, A. Akgerman, Z. Feng, Ind. Eng. Chem. Res. 36 (1997) 2580.
[29] H. Schulz, H. Gokcebay, in: J.R. Kosak (Ed.), Catalysis of Organic Reactions, Marcel Dekker, New York, 1984, pp. 153–169.
[30] H. Schulz, M. Claeys, Appl. Catal. A 186 (1999) 71.
[31] K.R. Krishna, A.T. Bell, J. Catal. 139 (1993) 104.
[32] T.J. Donnelly, C.N. Satterfield, Appl. Catal. A 52 (1989) 93.
[33] D.B. Bukur, S.A. Patel, Appl. Catal. A 61 (1990) 329.
[34] G.P. Van der Laan, Ind. Eng. Chem. Res. 38 (1999) 1277.
[35] H. Schulz, E. van Steen, M. Claeys, Stud. Surf. Sci. Catal. 81 (1994) 455.
[36] J.T. Kummer, T.W. Dewitt, P.H. Emmett, J. Am. Chem. Soc. 70 (1948) 3632.
[37] W.K. Hall, R.J. Kokes, P.H. Emmett, J. Am. Chem. Soc. 79 (1957) 2983.
[38] G. Blyholder, P.H. Emmett, J. Phys. Chem. 64 (1960) 470.
[39] H. Pichler, H. Schulz, Chem. Ing. Tech. 42 (1970) 1162.
[40] H. Schulz, A. Zeinel Deen, Fuel Proc. Tech. 1 (1977) 45.
[41] L.M. Tau, R. Robinson, R. Dudley Ross, B.H. Davis, J. Catal. 105 (1987) 335.
[42] B.S. Wu, L. Bai, H.W. Xiang, Y.W. Li, Z.X. Zhang, B. Zhong, Fuel 83 (2004) 205.
[43] R.J. Madon, S.C. Reyes, E. Iglesia, J. Phys. Chem. 95 (1991) 7795.
[44] R.B. Anderson, in: P.H. Emmett (Ed.), Catalysis, vol. IV, Van Nostrand-reinhold, New York, 1956, pp. 29–255.
[45] G. Henrici-Olivé, S. Olivé, Angew. Chem. 88 (1976) 144.
[46] R.B. Anderson, B. Seligman, J.F. Shultz, R. Kelly, M.A. Elliott, Ind. Eng. Chem. 44 (1952) 391.
[47] D.K. Matsumoto, C.N. Satterfield, Energy Fuels 3 (1989) 249.
[48] H. Schulz, M. Claeys, Appl. Catal. A 186 (1999) 91.
[49] E. Iglesia, S.C. Reyes, R.J. Madon, J. Catal. 129 (1991) 238.
[50] W.H. Zimmerman, D.B. Bukur, S. Ledakowicz, Chem. Eng. Sci. 47 (1992) 2707.
[51] E.W. Kuipers, I.H. Vinkenburg, H. Oosterbeek, J. Catal. 152 (1995) 137.
[52] F.P. Disanzo, J.L. Lane, P.M. Bergquist, S.A. Mooney, B.G. Wu, J. Chromatogr. 281 (1983) 101.
[53] Y. Yang, H.W. Xiang, Y.Y. Xu, L. Bai, Y.W. Li, Appl. Catal. A 266 (2004) 181.
[54] G.A. Huff, C.N. Satterfield, J. Catal. 85 (1984) 370.
[55] D.B. Bukur, X. Lang, D. Mukesh, W.H. Zimmerman, M.P. Rosynek, C. Li, Ind. Eng. Chem. Res. 29 (1990) 1588.